Extended Abstracts of the 2018 International Conference on Solid State Devices and Materials, Tokyo, 2018, pp869-870

Identification of different gas-phase reaction modes of WF_6 with SiH_4 for deposition of WSi_n films: powder formation and WSi_n cluster synthesis

Naoya Okada, Noriyuki Uchida, Shinichi Ogawa, and Toshihiko Kanayama
National Institute of Advanced Industrial Science and Technology (AIST)
1-1-1, Umezono, Tsukuba, Ibaraki, 305-8568, Japan Phone: +81-29-861-2512 E-mail: okada-naoya@aist.go.jp

Abstract

We elucidate the comprehensive mechanism of gas-phase reactions of WF_6 with SiH_4 for formation of WSi_n ($0 < n \leq 12$) films. Three gas-phase reaction modes are clearly identified depending on the partial pressure ratio of SiH_4 to WF_6: (1) powder formation, (2) Fluorine reduction, and (3) W-atom-encapsulated Si_n cage clusters synthesis modes. These findings enable us to precisely control the deposited film properties with definite Si and F contents while inhibiting the powder formation.

1. Introduction

For decades, W and W silicides (WSi_n) have been used as electrode materials in Si LSIs because of their low resistivity and high reliability. It is well known in the CVD of these films using SiH_4 and WF_6 source gases that the reaction mechanism drastically changes from a surface reaction to a gas-phase reaction at a partial pressure ratio of SiH_4 to WF_6 ($PR_{SiH4/WF6}$) = ~1.[1] Accordingly, deposition rates and film properties distinctively vary. Although the gas-phase reaction leads to a high deposition rate, this mode has a concern about powder generation.[1] By the use of the gas-phase reaction, Saito *et al.* showed that the Si content of WSi_n films can be increased to $n <$ ~3.[2, 3] However, what modes are present in the gas phase reactions remain to be elucidated.

In contrast, we demonstrated the formation of WSi_n films with much higher Si contents, up to $n \leq 12$ by preforming W-atom-encapsulated Si_n cage clusters in the gas phase: *i.e.*, the cluster-preforming deposition (CPD) method.[4] The WSi_n (n = 12) film exhibits particularly useful properties as a contact material for source/drain in Si CMOS: a reduction of the electron Schottky barrier height to 0.32 eV at W/WSi_n/n-type Si, excellent barrier properties against Cu diffusion, and an excellent contact hole coverage.[5] A question remains as to why the CPD is free from the power formation.

In this work, we identify that the three different modes are present in the gas-phase reactions of SiH_4 and WF_6; *i.e.*, powder formation mode, Fluorine (F) reduction mode, and W-atom-encapsulated Si_n ($n \geq 6$) cage cluster synthesis mode.

2. Experimental

The WSi_n film was prepared using SiH_4 and WF_6 on a SiO_2/Si substrate by a cold wall CVD (FIG. 1 (a)) or a hot-wall CPD system (FIG. 1 (b)). The number density of powders formed the film, N_P was estimated from dark field images of optical microscope (OM) and scanning electron microscope (SEM) images over an area of ~1 mm^2. The substrate stage temperature T_S was set to 260−400 ˚C. SiH_4 and WF_6 were introduced into the reactor at a mass flow rate of 0.2−1 SCCM and 0.01−0.2 SCCM, respectively, and the gas pressure was maintained at a total pressure P_T of 10 Pa (TABLE 1). For CPD, hydrogenated W-atom-encapsulated WSi_nH_x ($n \leq 12$) clusters are preformed by reaction of WF_6 and SiH_4 in the gas phase and then deposited onto a substrate. On the substrate surface heated at T_S =350−400 ˚C, WSi_nH_x clusters are thermally dehydrogenated and coalesce to the WSi_n film with less hydrogen content.[4]

2. Powder formation mode in CVD

As $PR_{SiH4/WF6}$ increased > 1, the n value of the WSi_n film drastically increased (FIG. 2).[1] This indicates the reaction mechanism of SiH_4 and WF_6 changes from the surface reaction to the gas-phase reaction. Accordingly, the film morphology also changed (FIG. 3 (a) and (b)), and N_P peaked near the onset of gas-phase reaction (FIG. 4). This behavior indicates that the powder generation is due to the high reactivity of WF_6 with SiH_4 in the gas phase. In fact, the reaction of WF_6 and SiH_4 starts at a low temperature ~120 ˚C. Once a WF_6 molecule is reduced by a SiH_4 with HF detachment to an even more reactive WF_5, it collides with another SiH_4 to produce an adduct $WF_y(SiH_x)_n$ ($y \leq 5$, $n < 6$). These adduct clusters are highly reactive with each other, enabling the rapid polymerization reaction accompanied with HF desorption if they are allowed to collide with other clusters or WF_6 molecules. This polymerization reaction continues as far as the product cluster contains F, resulting in the formation of powders by chain reactions among these reactive clusters.

3. Fluorine reduction mode in CVD

When $PR_{SiH4/WF6}$ exceeded ~100, the film morphology did not change (FIG. 3 (b) and (c)) but N_P decreased gradually with increasing $PR_{SiH4/WF6}$. This is because the collision frequency between the $WF_y(SiH_x)_n$ clusters and SiH_4 increases with $PR_{SiH4/WF6}$; consequently, the clusters lose the F content y with the increase of n, resulting in the lower reactivity of the product clusters. Furthermore, the reactivity drops drastically when $n \geq 6$ and $y = 0$: WSi_nH_x ($n \geq 6$) clusters. In fact, the WSi_n film does not reach $n = 6$ even when $PR_{SiH4/WF6} >$ ~1000.

4. WSi_nH_x ($n \geq 6$) cluster synthesis mode in CPD

Under the CPD condition of an extremely high $PR_{SiH4/WF6}$, sufficient times of collisions between the $WF_y(SiH_x)_n$ cluster and SiH_4 molecules are provided. The resulting film is in an amorphous state (FIG. 3 (d)), which is densely packed with clusters without vacancy and void (FIG. 5), with very few residual F of < ~0.1 at. % (FIG. 6) because of the sufficient reduction reaction with SiH_4 in the gas phase. This value is much lower than that in a conventional CVD film of > ~1

at. %. The n value of the clusters was determined by the gas temperature (FIG. 7), indicating that the energy barrier for reaction between the WSi_nH_x cluster and SiH_4 increases with n. Therefore, the reaction probability is very low when WSi_nH_x ($n \geq 6$) clusters collide each other in the gas phase, resulting in the almost complete inhibition of the powder generation. This suppression becomes more when n is saturated near 12 because $WSi_{12}H_x$ cluster is the most stable final product.

5. Conclusions

We demonstrated the presence of three reaction modes in the gas phase of SiH_4 and WF_6 well-separated as a function of $PR_{SiH4/WF6}$.

1. Near the onset of the gas-phase reaction turning from the surface reaction, the product species contains appreciable F amounts and "Powder formation mode" dominates.
2. Under the condition of $PR_{SiH4/WF6} > \sim 10$, the sufficient reaction with SiH_4 molecules reduces the F content in the product; *i.e.*, "F reduction mode", where the powder formation is inhibited as $PR_{SiH4/WF6}$ increases due to the less reactivity of the product.
3. Only under the condition of an extremely high $PR_{SiH4/WF6}$, "WSi_nH_x ($n \geq 6$) cluster synthesis mode" is available.

Our work provides a guideline for the CVD and CPD WSi_n films using the gas-phase reactions of WF_6 with SiH_4.

TABLE 1. Deposition conditions of WSi_n-CVD

SiH_4 (SCCM)	WF_6 (SCCM)	$PR_{SiH4/WF6}$	P_T (Pa)	T_S (°C)	Deposition time (min)
0.2	0.2	1	10	300	10
0.6	0.2	3	10	300	10
1.0	0.2	5	10	300	10
2.0	0.2	10	10	300	10
5.0	0.05	100	10	300	40
5.0	0.01	500	10	300	60

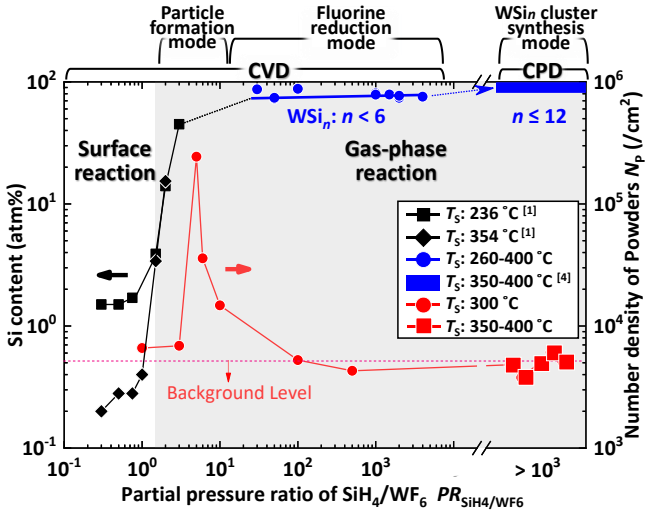

FIG. 2. Si content of the WSi_n film and number density of powders N_P on the substrate after CVD and CPD processes as a function of partial pressure ratio of SiH_4 to WF_6, $PR_{SiH4/WF6}$.

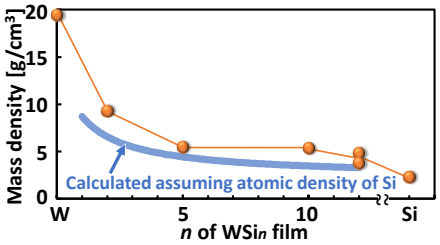

FIG. 5 Mass density of the resulting WSi_n films, estimated by X-ray reflectivity analysis, as a function of composition n. The blue curve is the mass density assuming the same atomic density as that of Si, indicating that the film has an atomic density higher than Si.

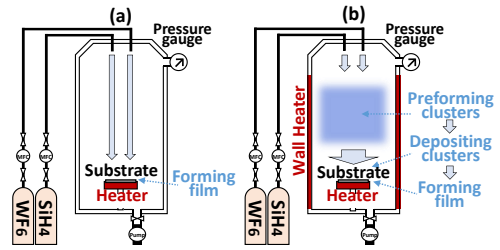

FIG. 1. Schematic of (a) cold wall CVD and (b) CPD systems for the WSi_n film

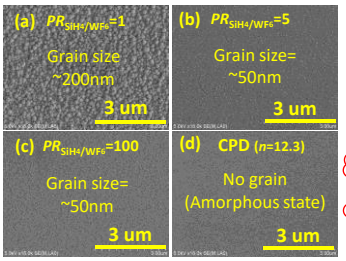

FIG. 3. SEM images of the film morphology prepared by CVD under (a) $PR_{SiH4/WF6} = 1$, (b) 5, (c) 100, and (d) CPD conditions

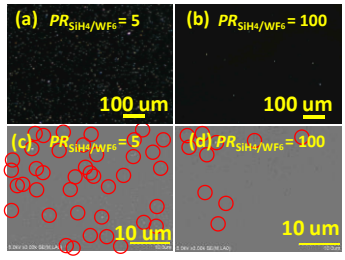

FIG. 4. Dark field OM images (a, b) and SEM images (c, d) of powders on the substrate after CVD of $PR_{SiH4/WF6} = 5$ (a, c) and 100 (b, d)

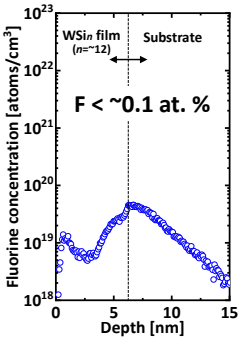

FIG. 6. SIMS depth profile of the residual fluorine (F) in the WSi_n film with n =12

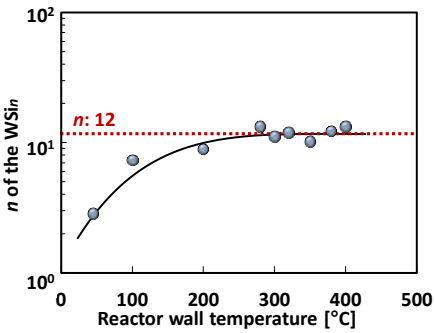

FIG. 7. Composition ratio n of the WSi_n film prepared by CPD as a function of the reactor wall temperature. Other conditions were fixed.

References

[1] M. Suzuki, *et al.*, *J. Electrochem. Soc.*, **137**, 3213 (1990).
[2] T. Saito, *et al.*, *Jpn. J. Appl. Phys.*, **33**, 275 (1994).
[3] T. Saito, *et al.*, *Chemical Engineering Science*, **62**, 6403 (2007).
[4] N. Okada, *et al.*, *J. Chem. Phys.*, **144**, 084703 (2016).
[5] N. Okada, *et al.*, *IEDM*, **22.5**, (2017).